Eur. Phys. J. B **16**, 261–268 (2000)

THE EUROPEAN PHYSICAL JOURNAL B

EDP Sciences

Antiferromagnetism in a doped spin-Peierls model: Classical and quantum behaviors

R. Mélin[a]

Centre de Recherches sur les Très Basses Températures (CRTBT)[b], CNRS, BP 166X, 38042 Grenoble Cedex, France

Received 9 December 1999

Abstract. We address the problem of antiferromagnetism in a two-dimensional model of doped spin-Peierls system, at the classical and quantum levels. A Bethe-Peierls solution is derived for the classical model, with an ordering temperature proportional to the doping concentration. The quantum model is treated in a cluster renormalization group showing a finite randomness behavior and an antiferromagnetic susceptibility at low temperature.

PACS. 75.10.Jm Quantized spin models – 75.50.Ee Antiferromagnetics

1 Introduction

The spin-Peierls transition at $T_{\rm SP} \simeq 14$ K in the inorganic quasi one-dimensional spin-Peierls compound $CuGeO_3$ has attracted much interest [1]. This transition is characterized by the appearance of a finite dimerization in the CuO_2 chains, and the opening of a spin gap. With $CuGeO_3$, it became possible to experiment the effect of doping in a spin-Peierls system. An antiferromagnetic (AF) phase was discovered upon replacing a fraction of the Cu ions (with $S = 1/2$) by magnetic ions with a different spin: Ni [2] (with $S = 1$) or Co [3] (with $S = 3/2$), or non magnetic ions: Zn [4–6] or Mg [7]. Also, the Ge sites (outside the CuO_2 chains) can be substituted with Si [8], leading to antiferromagnetism at low temperature.

Recent experiments by Manabe *et al.* have shown the existence of a finite Néel temperature $\simeq 25$ mK, with a doping concentration as low as 0.12% [9]. The doping dependence of the Néel temperature obtained in these experiments suggests the absence of a critical concentration for the appearance of antiferromagnetism: at low doping the ordering temperature scales like $\ln T_{\rm N} \propto 1/x$ [9].

Early theoretical works [10–12] have focussed on the identification of the relevant low energy degrees of freedom. Fukuyama, Tanimoto and Saito [11] have shown the coexistence between antiferromagnetism and dimerization in a doped spin-Peierls model. The degrees of freedom relevant to the low energy physics are solitonic spin-1/2 excitations pinned at the impurities [12]. These excitations are the building blocks of the theory in references [13–15]. These spin-1/2 objects interact *via* an exchange decaying exponentially with distance. Interchain interactions can be incorporated by considering the existence of a transverse correlation length, approximately one tenth of the longitudinal correlation length, as recently proposed independently by Dobry *et al.* [16], and Fabrizio, Mélin and Souletie [15]. Numerical calculations with realistic spin-phonon couplings have provided a link between the microscopic Hamiltonian and the effective model of interacting spin-1/2 moments [10,17–20]. The approach followed in references [13–15] and continued in the present work relies on the treatment of disorder in the effective Hamiltonian. This allows to discuss the qualitative physics of large scale systems at a finite temperature, while the numerical methods have so far been limited to the ground state properties [10,16–20]. The effective Hamiltonian is unfrustrated because of the staggered exchanges. As we show, it is remarkable that frustration is not generated by coarse graining the model while the low energy Hamiltonian is controlled by a finite randomness fixed point [21]. This may be contrasted with spin glasses, also controlled by a finite randomness fixed point, but in which frustration plays a relevant role. The scope of this article is to analyze the model beyond the percolation approximation used in reference [15], both at the classical and quantum levels. We first show in Section 3 that the physics of the quantum Hamiltonian is already present in the classical Ising Hamiltonian, and give a rigorous derivation of mean field theory *via* a Bethe-Peierls treatment. The second purpose of the article is to show that the quantum Hamiltonian has an antiferromagnetic behavior at low temperature. The quantum model is treated in a cluster renormalization group (RG) calculation in Sections 4 and 5.

[a] e-mail: melin@labs.polycnrs-gre.fr
[b] UPR 5001 du CNRS, Laboratoire conventionné avec l'Université Joseph Fourier

2 The model

We recall the model proposed in reference [13]. When impurities are introduced in a dimerized background (for instance non magnetic impurities such as Zn), spin-1/2 solitonic moments are released out of the dimerized pattern. These magnetic moments are pinned at the impurities due to interchain interactions [12]. This picture is in agreement with susceptibility experiments [9,22,23], indicating the release of one spin-1/2 moment per Zn impurity at low doping. The interaction between two magnetic moments at a distance d originates from virtual excitations of the gaped dimerized background, and decays exponentially with distance, with a characteristic length set by the correlation lengths $\xi_x \sim 9c$ along the chain direction (c-axis) [24,25], and $\xi_y \sim \xi_x/10$ in the b-axis direction. These exchange interactions as well as the relevance of disorder were identified in reference [13] to play a crucial role in the establishment of antiferromagnetism. The low energy physics of a doped spin-Peierls system is represented by spin-1/2 solitonic magnetic moments distributed at random with a concentration x on a square lattice, and interacting *via* a Heisenberg Hamiltonian [15,16]

$$H = \sum_{\langle i,j \rangle} J_{i-j} \mathbf{S}_i \cdot \mathbf{S}_j, \tag{1}$$

the exchange in equation (1) being staggered and decaying exponentially with distance:

$$J_{i-j} = (-1)^{d_x+d_y+1} \Delta \exp\left(-\sqrt{\left(\frac{d_x}{\xi_x}\right)^2 + \left(\frac{d_y}{\xi_y}\right)^2}\right), \tag{2}$$

with $\xi_x \simeq 9c$ the correlation length along the c-axis and $\xi_y \simeq 0.1 \times \xi_x$ the correlation length along the b-axis. Correlations along the a-axis are neglected.

3 Classical Ising model

We consider a model with Ising degrees of freedom, distributed randomly and interacting *via* the exchange in equation (2). The classical antiferromagnet has the same transition temperature as the classical ferromagnet. We consider therefore the ferromagnetic model to calculate the ordering temperature.

3.1 One-dimensional model

A high temperature expansion leads to the exact form of the correlations in terms of a product over the bonds between the spins at sites 0 and L: $\langle \sigma_0 \sigma_L \rangle = \prod \tanh(\beta J_{i,i+1})$. We calculated numerically the disorder average to obtain the correlation length at a finite temperature. As shown in Figure 1, the average correlation length of the disordered model is larger than the typical correlation length $\xi = -1/[x \ln(\tanh(\beta T^*))]$, with $T^* = \Delta \exp(-1/(x\xi))$ the exchange of the particular disorder realization where the magnetic moments are equally spaced. We calculated in reference [14] the correlation length of the quantum chain and found a similar result: the enhancement of the magnetic correlations above T^* due to disorder does not rely on the quantum nature of the coupling Hamiltonian in spite of a random singlet physics in the quantum chain, not present in the Ising chain.

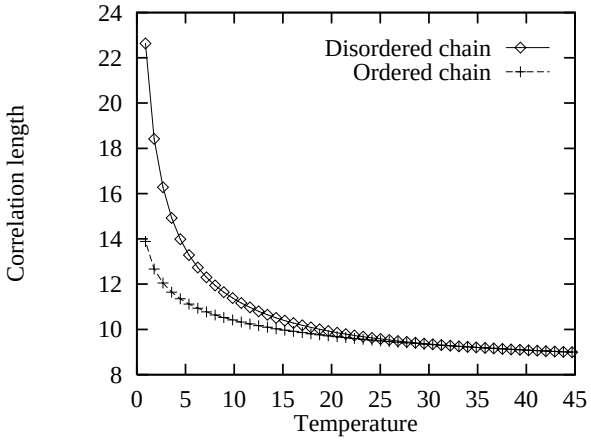

Fig. 1. The average correlation length of the disordered Ising spin chain with nearest neighbor couplings is larger than the correlation length of an ordered system with the same concentration $x = 0.01$ above T^*. We used $\Delta = 44.7$ K, $\xi = 9$.

3.2 Determination of the exchange distribution

We consider the exchanges to be drawn independently in a distribution $P(J)$ resulting from the combination of randomness in the spatial distribution of the magnetic moments and exponentially decaying interactions (Eq. (2)). The relevant exchanges are set by the spins the closest to each other. Therefore, given a spin at site (x_0, y_0), we need to determine the probability that one spin is found on the periphery of the ellipse $[(x-x_0)/\xi_x]^2 + [(y-y_0)/\xi_y]^2 = \gamma^2$, with no other spin inside the ellipse, and therefore an exchange $\Delta \exp(-\gamma)$. We consider a system of total area A containing n spins. The probability to find no spin inside a subsystem of area δA is $P_0 = \left(1 - \frac{\delta A}{A}\right)^n \simeq \exp(-x\delta A)$, with $x = n/A$ the doping concentration. Now the spacing distribution is

$$P(\gamma) = xL(\gamma) \exp(-x\delta A(\gamma)), \tag{3}$$

with $L(\gamma) = \mathrm{d}[A(\gamma)]/\mathrm{d}\gamma$. In the one-dimensional model, we have $\delta A(\gamma) = 2\gamma\xi_x$, and $L(\gamma) = 2\xi_x$. In the two-dimensional isotropic model with $\xi_x = \xi_y = \xi$, we have $\delta A(\gamma) = \pi\gamma^2\xi^2$, and $L(\gamma) = 2\pi\gamma\xi$. In the quasi one-dimensional model, $\delta A(\gamma) = \pi\gamma^2\xi_x\xi_y$, and $L(\gamma) = 2\pi\gamma\xi_x\xi_y$. The distribution $P(\gamma)$ of the isotropic and anisotropic two-dimensional models is a Wigner distribution with a short scale "distance repulsion". This repulsion will be shown not to affect the ordering properties.

3.3 Bethe-Peierls transition in the infinite coordination limit

We now consider the Bethe-Peierls solution of the Ising model [26]. The lattice has a tree topology, with a forward branching ratio $z-1$, and we calculate the magnetization of the site with the highest hierarchical level (top spin), in the presence of the other sites. We consider $z-1$ trees and connect them to obtain a tree with one more generation (see Fig. 2). The recursion of the average magnetization of the top spin reads [27]

$$X=\frac{\prod_{i=1}^{z-1}(1+Y_i\tanh(\beta J_i))-\prod_{i=1}^{z-1}(1-Y_i\tanh(\beta J_i))}{\prod_{i=1}^{z-1}(1+Y_i\tanh(\beta J_i))+\prod_{i=1}^{z-1}(1-Y_i\tanh(\beta J_i))}, \tag{4}$$

where Y_i, $i=1,...,z-1$ are the magnetizations of the top spins with n generations, and X the magnetization of the top spin with $n+1$ generations. We first consider the artificial situation where the ordering temperature is large compared to the exchange: $T_{\rm bp}\gg\Delta$, which turns out to be equivalent to assuming a large coordination. Equation (4) is linearized into $X=\sum_{i=1}^{z}Y_i\tanh(\beta J_i)$, leading to the recursion of the magnetization $\langle\langle X\rangle\rangle_{n+1}=(z-1)\langle\langle\tanh(\beta J)\rangle\rangle\langle\langle X\rangle\rangle_n$, with the subscript n labeling the number of generations. This leads to the ordering temperature $T_{\rm bp}=(z-1)\langle\langle J\rangle\rangle$, far above Δ if $z\gg1$, and consistent with the initial assumption. We can calculate the ordering temperature $T_{\rm bp}$ with the different distributions $P(J)$ derived in Section 3.2. We find:

(i) *with the one-dimensional model distribution*: $T_{\rm bp}=2(z-1)x\xi\Delta/(1+2x\xi)$;
(ii) *with the isotropic two-dimensional model distribution*: $T_{\rm bp}\simeq2(z-1)\pi x\xi^2\Delta$ in the dilute regime $x\xi^2\ll1$.
(iii) *with the quasi one-dimensional model distribution*: $T_{\rm bp}\simeq2(z-1)\pi x\xi_x\xi_y\Delta$ in the dilute regime $x\xi_x\xi_y\ll1$.

The three limits therefore show a similar behavior $T_{\rm bp}\propto(z-1)x\Delta$, showing that the short distance Wigner repulsion in the spacing distribution equation (3) does not affect the ordering properties. Comparing the Bethe-Peierls ordering temperature to the ordering temperature obtained from the Stoner criterion in reference [15], we see that $z-1$ should be identified with the interchain coupling. The small-z regime, relevant to weak interchain correlations, is now discussed in Sections 3.4 and 3.5.

3.4 Bethe-Peierls transition with a finite coordination: (i) Percolation approximation

We now consider the physics at a finite $z=3$. In this regime, the Bethe-Peierls method takes into account the inhomogeneities of the magnetization, not included in the Stoner criterion mean field solution in reference [15]. We first consider a "percolation approximation" in which we assume the bonds $J\ll T$ ($J\gg T$) to be set to zero

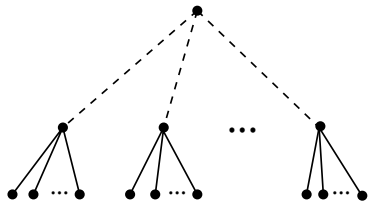

Fig. 2. The tree structure used in the Bethe-Peierls calculation. The forward branching ratio is $z-1$. A tree with $n+1$ generations is obtained from connecting $z-1$ trees with n generations.

(infinity) in the effective percolation problem. With $z=3$, the Bethe-Peierls iteration equation (4) reads

$$X=\frac{Y\tanh(\beta J_y)+Z\tanh(\beta J_z)}{1+YZ\tanh(\beta J_y)\tanh(\beta J_z)},$$

and is approximated into: (i) $T\ll J_y, T\ll J_z$: $X\simeq Y+Z$; (ii) $T\gg J_y$, $T\ll J_z$: $X\simeq Z$; (iii) $T\ll J_y$, $T\gg J_z$: $X\simeq Y$; (iv) $T\gg J_y, T\gg J_z$: $X\simeq0$. The recursion of the average magnetization is therefore $\langle\langle X\rangle\rangle_{n+1}\simeq2\lambda\langle\langle X\rangle\rangle_n$, with the percolation parameter

$$\lambda=\int_T^{+\infty}P(J){\rm d}J. \tag{5}$$

With the one-dimensional distribution, we have $\lambda=1-(T/\Delta)^{2x\xi_x}$, which yields a transition at the temperature

$$T^*=\Delta\exp\left(-\frac{2\ln2}{x\xi_x}\right), \tag{6}$$

exponentially small in $1/(x\xi_x)$. This behavior is compatible with reference [15] where we have shown the absence of a true ordering transition in the percolation approximation of a two-dimensional anisotropic model, while the model was shown to percolate in a finite size.

3.5 Bethe-Peierls transition with a finite coordination: (ii) Beyond the percolation approximation

We now solve the Ising model beyond the percolation approximation. We take into account the iteration of small exchanges to lowest order, with the following approximate iteration: (i) $T\ll J_y$, $T\ll J_z$: $X\simeq Y+Z$; (ii) $T\gg J_y$, $T\ll J_z$: $X\simeq\beta J_yY+Z$; (iii) $T\ll J_y$, $T\gg J_z$: $X\simeq Y+\beta J_zZ$; (iv) $T\gg J_y$, $T\gg J_z$: $X\simeq\beta J_yY+\beta J_zZ$. The dominant contribution originates from the region (iv) of the couplings: $\langle\langle X\rangle\rangle_{n+1}\simeq(2/T)\mu(1-\lambda)\langle\langle X\rangle\rangle_n$, with λ in equation (5), and $\mu=\int_0^T JP(J){\rm d}J$. With the one-dimensional distribution for $P(J)$, we have $\mu\simeq2x\xi\Delta$ and therefore the same critical temperature $T_{\rm bp}=4x\xi\Delta$ as in the model with a large connectivity z (with $z=3$ in this calculation). It is remarkable that the correct treatment of the small exchanges restores a transition temperature $\propto x\xi\Delta$. This shows the relevant role played by energy scales smaller than the temperature.

The main unsolved question regarding the classical model behavior is to determine whether the finite dimensional model has a true thermodynamic transition at

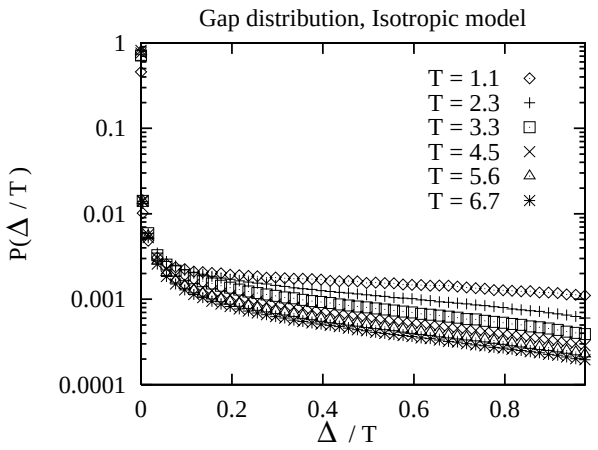

Fig. 3. Evolution of the gap distribution of the model with isotropic exchanges $\xi_x = \xi_y = 9$, $\alpha = 2$ as the temperature is scaled down. The doping concentration is $x = 0.01$ and the system has a size 200×200. The weight of energy scales $\sim T$ increases as the temperature is decreased.

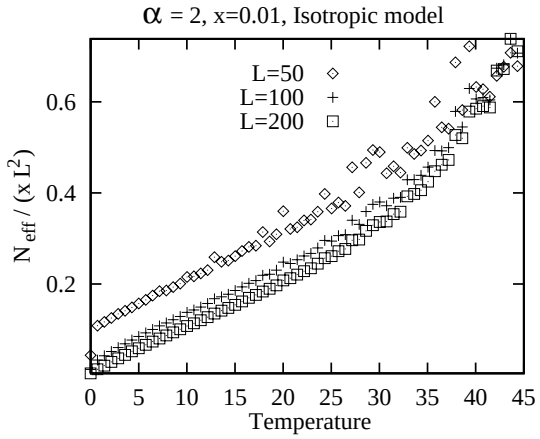

Fig. 4. Temperature dependence of the number of effective moments, normalized to the number of initial moments xL^2. We have set $\xi_x = \xi_y = 9$, $\Delta = 44.7$ K, $x = 0.01$, $\alpha = 2$. We used square systems of dimensions $L \times L$, with $L = 50$ ($\Diamond$), $L = 100$ ($+$), and $L = 200$ ($\Box$). For large system sizes, $N_{\rm eff} \sim (T/\Delta)xL^2$.

a temperature $\propto x\xi\Delta$. The Bethe-Peierls solution orders at a temperature $\propto x\xi\Delta$ because of the strong short range correlations. This does not necessarily mean that the finite dimensional model also has a true thermodynamic transition at this temperature. Instead, we believe it possible that the classical model has a cross-over to a Griffiths physics at a temperature $\propto x\xi\Delta$ and a true thermodynamic transition with a diverging correlation length at a temperature T^*, which would also be a behavior compatible with a low temperature antiferromagnetic susceptibility. At the present stage, we cannot make the distinction between these two behaviors.

4 Quantum isotropic model

We first consider the artificial situation where the correlation lengths are identical in the two directions: $\xi_x = \xi_y = \xi = 9$. The tendency to ordering in this isotropic model is overestimated compared to the anisotropic model with $\xi_x = 9$, $\xi_y = 0.1 \times \xi_x$. We are led to consider the class of interactions

$$J_{i-j}=(-1)^{d_x+d_y+1}\Delta \exp\left(-\left[\left(\frac{d_x}{\xi_x}\right)^2+\left(\frac{d_y}{\xi_y}\right)^2\right]^{\alpha/2}\right), \tag{7}$$

decaying faster than the interactions in equation (2) if $\alpha > 1$. The cluster RG (see the Appendix) generates large energy scales in the parameter range $\alpha < \alpha_0 \simeq 1.2$. It turns out that $\alpha_0 < 1$ in the model with anisotropic exchanges, and we therefore consider only the regime $\alpha > \alpha_0 \simeq 1.2$ in the isotropic model.

The gap distribution is shown in Figure 3 for decreasing temperatures. It is visible that the RG produces gaps of order of the temperature T unlike in the case of the infinite randomness fixed point where the opposite occurs (see Ref. [28] for the one-dimensional Heisenberg chain with an infinite randomness, random singlet behavior; see reference [21] for the infinite randomness behavior in the two-dimensional Ising model in a transverse field). As in the Ising model analysis, we calculate the susceptibility in two ways: (i) we assume a paramagnetic behavior of the set of effective moments; (ii) we incorporate the correlations induced by exchanges $\Delta \sim T$, in which case an antiferromagnetic behavior in the susceptibility is restored.

4.1 Infinite randomness calculation

We first consider all the exchanges $J < T$ to be set to zero: the set of effective spins is viewed as a paramagnet with a susceptibility

$$\chi = \frac{1}{TL^2}\langle\langle \sum_{i=1}^{N^{(\rm eff)}} S_i^{(\rm eff)}(S_i^{(\rm eff)}+1)\rangle\rangle, \tag{8}$$

where $N^{(\rm eff)}$ the number of effective spins. We have discarded a prefactor 1/3 in equation (8), not relevant to the present calculation. The low temperature susceptibility is therefore controlled by two quantities: (i) the density of free spins $n_{\rm eff} = \langle\langle N^{(\rm eff)}\rangle\rangle/(xL^2)$; and (ii) the magnitude of the effective spin.

The number of effective moments scales like $N_{\rm eff} \sim (T/\Delta)xL^2$, as it is visible in Figure 4. The squared effective moment shows two regimes:

(i) *High temperature regime*: The high temperature average squared effective moment scales like $\langle\langle[S^{\rm eff}]^2\rangle\rangle \sim \Delta/T$ (see Fig. 5). The susceptibility per unit volume is $\chi \sim x/T$.

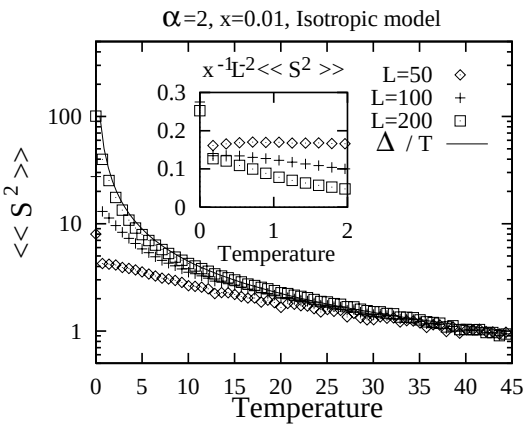

Fig. 5. Temperature dependence of the the average square effective moment $\langle\langle[S^{\rm eff}]^2\rangle\rangle$ with $\xi_x = \xi_y = 9$, $\Delta = 44.7$ K, $x = 0.01$, $\alpha = 2$. We used square systems of dimensions $L \times L$, with $L = 50$ ($\Diamond$), $L = 100$ ($+$), $L = 200$ ($\Box$). The solid line is Δ/T. The insert shows the low temperature dependence of $(xL^2)^{-1}\langle\langle[S^{\rm eff}]^2\rangle\rangle$.

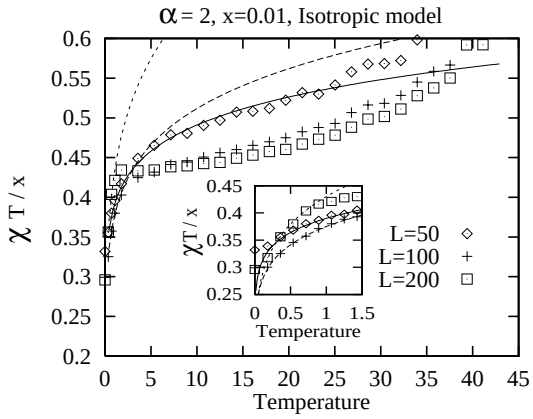

Fig. 6. Temperature dependence of the Curie constant $T\chi(T)/x$ with $\xi_x = \xi_y = 9$, $\Delta = 44.7$ K, and for $\alpha = 2$. We used square systems of dimension $L \times L$, with $L = 50$ ($\Diamond$), $L = 100$ ($+$), $L = 200$ ($\Box$). The low temperature regime has been fit to a power law behavior $\chi T/x = 0.39 \times T^{-0.1}$ ($L = 50$, solid line), $\chi T/x = 0.375 \times T^{0.135}$ ($L = 100$, long dashed line), and $\chi T/x = 0.43 \times T^{0.18}$ ($L = 200$, short dashed line). The insert shows the low temperature behavior.

(ii) *Low temperature percolation regime*: At low temperature, the squared effective moment scales like $\langle\langle S^2\rangle\rangle \sim axL^2$, with a some constant (see the insert Fig. 5). The susceptibility per unit volume is $\chi \sim (ax^2L^2)/\Delta$. In this regime, a cluster has percolated through the finite size system. Its magnetization results from summing xL^2 variables $S_i^z = \pm 1/2$, corresponding to the two sublattices magnetizations. Therefore, $\langle\langle S\rangle\rangle \sim \sqrt{xL^2}$, and $\langle\langle S^2\rangle\rangle \sim xL^2$.

The cross-over between these regimes occurs at the temperature scale $T_{\rm co} = (\Delta/a)(xL^2)^{-1}$, which decreases to zero when the system size is increased. Therefore in the thermodynamic limit, only the high temperature paramagnetic behavior survives while in a finite size, a low temperature tail is present in the susceptibility (see Fig. 6). Now the situation changes when correlations between spins coupled by exchanges of order T are included.

4.2 Finite randomness calculation

To schematically incorporate the correlations at energy scales of order of the temperature, we consider as frozen the spins connected by an exchange with a gap between $T/2$ and T. This freezing results in a staggered magnetization because the set of effective moments is unfrustrated (see the Appendix). The resulting susceptibility is shown in Figure 7. It is visible that χT is linear in T at small T, with therefore a finite susceptibility at zero temperature. This shows qualitatively how an antiferromagnetic behavior can be restored because of the correlations at energy scales $\Delta \sim T$.

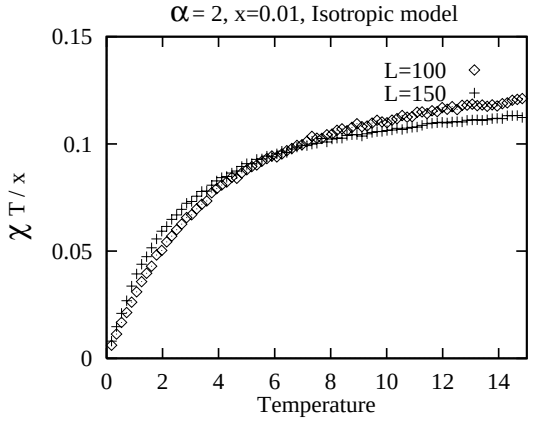

Fig. 7. Temperature dependence of the Curie constant $\chi T/x$ with an isotropic system of size $L \times L$, with $L = 100$, $L = 150$. The spins connected by exchanges between $T/2$ and T have been frozen. This results in a finite Curie constant at zero temperature.

5 Quantum anisotropic model

5.1 One-dimensional model

In one dimension, the RG equations of a model in which only AF nearest neighbor exchanges are retained can be solved exactly (see Ref. [14]). We note $x = J/[\mathrm{Max}(J)]$ the exchange normalized to the maximal exchange. The distribution of the variable x is $P(x) = (\overline{f}/\Gamma)x^{\overline{f}/\Gamma - 1}$, with $\Gamma = \ln(\Delta/\mathrm{Max}(J))$, and $\overline{f}/\Gamma = x\xi/(1 + \Gamma x\xi)$. The weight on the strongest exchanges $x \simeq 1$ is $\simeq x\xi$ above the cross-over temperature $T^* = \Delta \exp(-1/x\xi)$, and decreases to zero at temperatures below T^*, where the system has crossed over to the random singlet fixed point. As

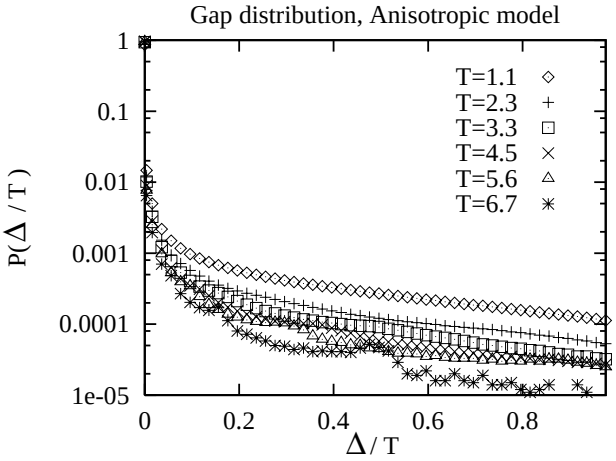

Fig. 8. Gap distribution of the anisotropic model, with $\xi_x = 9$, $\xi_y = 0.1 \times \xi_x$, and $x = 0.01$ and a system of size $L_x \times L_y$, with $L_x = 640$ and $L_y = 64$. The oscillatory behavior at high temperature is due to the anisotropy in the couplings.

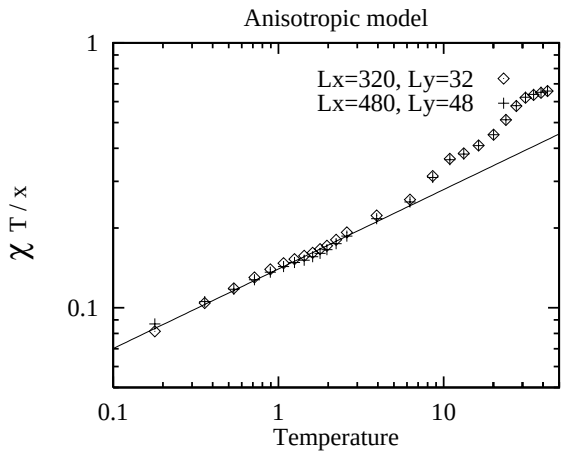

Fig. 9. Temperature dependence of the Curie constant $\chi T/x$ of the anisotropic model, with $\xi_x = 9$, $\xi_y = 0.1 \times \xi_x$, and $x = 0.01$. The lattice sizes are 320×32 and 480×48. The solid line is a fit of the low temperature behavior to the form $\chi T = 0.14 \times T^{0.3}$.

a test of our program, we considered the cluster RG of a one-dimensional model, with the exchanges not restricted to nearest neighbors (see Eqs. (1, 2)). For any practical temperature above T^*, the weight on energy scales of order T is found to remain constant as the system is renormalized, with therefore the same behavior as in the one-dimensional model with AF nearest neighbor exchanges only.

5.2 Anisotropic model

We show in Figure 8 the evolution of the gap distribution as the system is scaled down, with the parameters $\xi_x = 9$, $\xi_y = 0.1 \times \xi_x$, relevant to $CuGeO_3$. As in the isotropic model, energy scales of order T are generated upon renormalizing the system. To qualitatively include the effects of correlations at energy scales $\Delta \sim T$, we consider the spins connected by an exchange with a gap between $T/2$ and T to be frozen, and obtain a low temperature power-law Curie susceptibility, $\chi \sim T^{\alpha}$, with $\alpha = -0.7$ if $x = 0.01$ (see Fig. 9). The low temperature susceptibility diverges slower than a Curie law, which is a behavior characteristic of an antiferromagnet. We did not succeed to obtain $\alpha > 0$ as it is the case in doped $CuGeO_3$. Therefore, we cannot rigorously conclude on whether antiferromagnetism is long ranged or associated to a zero temperature transition. A precise discussion of this point is an open question, and would require the correlations at energy $\Delta \sim T$ to be incorporated beyond our present treatment. For instance the cluster RG could be used to renormalize the high energy physics and the low energy effective Hamiltonian could be treated by exact diagonalizations.

6 Conclusions

We have shown that the physics of the quantum Hamiltonian equations (1, 2) was already present at the level of the classical Ising model. A Bethe-Peierls treatment of the classical model has been given in which a transition at a temperature $\propto x\xi\Delta$ was found. The quantum Hamiltonian has been treated in a cluster RG. The model was shown to have a finite randomness behavior. We have shown at a qualitative level how a low temperature antiferromagnetic susceptibility can be obtained.

Two questions are left open:

(i) The Bethe-Peierls solution orders at a temperature $\propto x\xi\Delta$. We do not know whether the two-dimensional model has also a thermodynamic transition at a temperature $\propto x\xi\Delta$, or whether this temperature scale corresponds to a cross-over to a Griffith physics. Both behaviors would be *a priori* compatible with the existence of a maximum in the susceptibility of the antiferromagnet at a temperature $\propto x\xi\Delta$.

(ii) The quantum model susceptibility shows an antiferromagnetic behavior at low temperature due to correlations at energies $\Delta \sim T$. The isotropic model shows a finite susceptibility at low temperature while the quasi one-dimensional has a susceptibility diverging slower than a Curie law. A precise investigation of the low temperature susceptibility would require a treatment going beyond our present analysis, for instance by treating the low energy effective Hamiltonian by exact diagonalizations.

Two other proposals to explain antiferromagnetism in doped in $CuGeO_3$ have been made: Fukuyama, Tanimoto and Saito [11] and Mostovoy, Khomskii, and J. Knoester [29]. These proposals are quite different from ours, and we have exposed previously why we think our model is more relevant [15]. The inclusion of interchain interaction in our model in reference [15] and the present work, points strongly towards an compatibility with experiments.

The author thanks M. Fabrizio and J. Souletie for numerous fruitful discussions, their encouragements, and for useful comments on the manuscript. M. Fabrizio pointed out to me the possibility of cluster RG calculations as well as the proof that the effective problem remains unfrustrated as the system is scaled down. J. Souletie suggested the existence of a similar physics in the classical and quantum models. The cluster RG calculations have been performed on the CRAY T3E supercomputer of the Centre Grenoblois de Calcul Vectoriel of the Commisariat à l'Energie Atomique.

Note added in proof

The author has obtained an evidence that the classical model has a genuine thermodynamic transition, which will be the subject of a future publication.

Appendix A: Renormalization equations

We use a cluster RG to renormalize the quantum Hamiltonian equations (1, 2). The method relies on a perturbative expansion in the inverse of the largest exchange, and was originally proposed by Dasgupta and Ma [30] in the context of disordered Heisenberg chains. The cluster RG was applied by Bhatt and Lee [31] to a model of phosphorus doped silicon. Fisher used the method to solve exactly the random singlet fixed point [28]. The cluster RG was also used to investigate the low energy physics of disordered spin chains: the dimerized Heisenberg chain with random exchanges [32]; the spin-one chain with random exchanges [33,34]; Heisenberg chains with random ferromagnetic and antiferromagnetic couplings [35]. Recently, Motrunich *et al.* [21] shown the existence of an infinite randomness fixed point in two dimensions in the Ising model in a transverse field. At such a fixed point, inhomogeneities in the disorder grow indefinitely as the system is scaled down, as in the random singlet fixed point in one spatial dimension. We now give a short derivation of the RG equations.

We isolate two spins $\mathbf{S}_1$ and $\mathbf{S}_2$ coupled by an exchange J_{1-2}. This sets an energy scale given by the gap between the ground state and the first excited multiplet: if $J_{1-2} > 0$ is antiferromagnetic, the ground state has a spin $S = |S_1 - S_2|$ and the first excited multiplet has $S = |S_1 - S_2| + 1$, with a gap $\Delta_{1-2} = |J_{1-2}|(|S_1 - S_2| + 1)$. If $J_{1-2} < 0$ is ferromagnetic, the ground state has $S = S_1 + S_2$ and the first excited multiplet has $S = S_1 + S_2 - 1$, with a gap $\Delta_{1-2} = |J_{1-2}|(S_1 + S_2)$. Among all possible pairs of spins, we consider the one with the strongest gap Δ_{1-2}. This energy scale is identified to the system temperature. If $\mathbf{S}_1$ and $\mathbf{S}_2$ are coupled ferro ($J_{1-2} < 0$) , the two spins $\mathbf{S}_1$ and $\mathbf{S}_2$ are replaced by an effective spin $S = S_1 + S_2$. If they are coupled antiferro, they are replaced by an effective spin $S = |S_1 - S_2|$. $S_1 = S_2$ with an AF coupling J_{1-2} leads to singlet formation while a residual moment is formed otherwise.

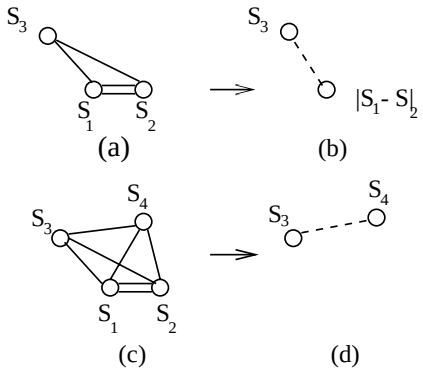

Fig. 10. The first RG transformations in a cluster expansion with a residual spin formation (a) and (b), and a singlet formation (c) and (d). The dashed lines represent renormalized exchanges.

A.1 Residual moment formation

Let us first consider the case where a residual moment is formed corresponding to (a) and (b) in Figure 10. We specialize a spin $\mathbf{S}_3$ among the other spins and denote by J_{i-j} the exchange between spins i and j, with $i, j = 1, ..., 3$. The coupling Hamiltonian between the spins $\mathbf{S}_1$ and $\mathbf{S}_2$ is $H_{1-2} = J_{1-2}\mathbf{S}_1 \cdot \mathbf{S}_2$ while the remaining couplings

$$H_I = J_{1-3}\mathbf{S}_1 \cdot \mathbf{S}_3 + J_{2-3}\mathbf{S}_2 \cdot \mathbf{S}_3 \tag{9}$$

are treated in a first order perturbation. This leads to the renormalized coupling Hamiltonian $H_I = \tilde{J}_3 \mathbf{S}_3 \cdot \mathbf{S}$, with the renormalized exchange

$$\tilde{J}_3 = J_{1-3}c(S_1, S_2, S) + J_{2-3}c(S_2, S_1, S), \tag{10}$$

with

$$c(S_1, S_2, S) = \frac{S(S+1) + S_1(S_1+1) - S_2(S_2+1)}{2S(S+1)}$$

derived in reference [35]. The sublattice on which the residual spin is placed is determined as follows: if $S_1 > S_2$, the residual spin S is placed on the same sublattice as S_1 while it is placed on the sublattice of S_2 if $S_1 < S_2$.

A.2 Singlet formation

We now consider singlet formation, with $S_1 = S_2$ coupled AF. The renormalized couplings are obtained in a second order perturbation theory. Generalizing the calculation in references [31,35] to the coupling Hamiltonian (9), we find the renormalized exchange

$$\tilde{J}_{3-4} = J_{3-4} + \frac{2S_1(S_1+1)}{3J_{1-2}}(J_{1-3} - J_{2-3})(J_{2-4} - J_{1-4}), \tag{11}$$

where $S_1 = S_2$ denote the spins at site 1 and 2. In the 1D limit $J_{2-3} = J_{1-4} = 0$ equation (11) reproduces the result in reference [35], and the spin-1/2 limit $S_1 = 1/2$ reproduces the result in reference [31].

A.3 Absence of frustration

We show that frustration is not generated by the RG procedure. We assume an unfrustrated starting Hamiltonian, and show that the different RG operations are compatible with the sublattice structure. We distinguish three cases:

(i) *S_1 and S_2 belong to different sublattices and are coupled antiferro.* We assume $S_1 > S_2$ and the effective spin $S = S_1 - S_2$ replaces the spin S_1. The renormalized coupling to another spin S_3 in equation (10) is

$$\tilde{J}_3 = J_{1-3} + (J_{1-3} - J_{2-3})\frac{S_2}{S+1}\cdot$$

$J_{1-3} > 0$ and $J_{2-3} < 0$ leads to $\tilde{J}_3 > 0$. $J_{1-3} < 0$ and $J_{2-3} > 0$ leads to $\tilde{J}_3 < 0$. The renormalized coupling $\tilde{J}_3$ has thus a sign compatible with the sublattice structure.

(ii) *S_1 and S_2 belong to the same sublattices and are coupled ferro.* J_{1-3} and J_{2-3} have the same sign. We have $c(S_1, S_2, S) > 0$ and $c(S_2, S_1, S) > 0$. The renormalized coupling $\tilde{J}_3$ has the same sign as J_{1-3} and J_{2-3}, compatible with the sublattice structure.

(iii) *$S_1 = S_2$ are coupled antiferro and a singlet is formed.* If S_3 and S_4 are coupled ferro and in the same sublattice, $\tilde{J}_{3-4} < 0$ in equation (11). If S_3 and S_4 are coupled antiferro and in the opposite sublattice, $\tilde{J}_{3-4} > 0$ in equation (11). The singlet formation is thus compatible with the sublattice structure.

References

1. M. Hase, I. Terasaki, K. Uchinokura, Phys. Rev. Lett. **70**, 3651 (1993); J.P. Pouget, L.P. Regnault, M. Ain, B. Hennion, J.P. Renard, P. Veillet, G. Dhalenne, A. Revcolevschi, Phys. Rev. Lett. **72**, 4037 (1994).
2. J.-G. Lussier, S.M. Coad, D.F. McMorrow, D. McK Paul, J. Phys. Cond. Matter **7**, L325 (1995).
3. P.E. Anderson, J.Z. Liu, R.N. Shelton, Phys. Rev. B **56**, 11014 (1997).
4. M. Hase, N. Koide, K. Manabe, Y. Sasago, K. Uchinokura, A. Sawa, Physica B **215**, 164 (1995).
5. M. Hase, K. Uchinokura, R.J. Birgeneau, K. Hirota, G. Shirane, J. Phys. Soc. Jpn **65**, 1392 (1996).
6. M.C. Martin, M. Hase, K. Hirota, G. Shirane, Phys. Rev. B **56**, 3173 (1997).
7. T. Masuda, A. Fujioka, Y. Uchiyama, I. Tsukada, K. Uchinokura, Phys. Rev. Lett. **80**, 4566 (1998).
8. J.-P. Renard, K. Le Dang, P. Veillet, G. Dhalenne, A. Revcolevschi, L.P. Regnault, Europhys. Lett. **30**, 475 (1995); L.P. Regnault, J.P. Renard, G. Dhalenne, A. Revcolevschi, Europhys. Lett. **32**, 579 (1995).
9. K. Manabe, H. Ishimoto, N. Koide, Y. Sasago, K. Uchinokura, Phys. Rev. B **58**, R575 (1998).
10. G.B. Martins, E. Dagotto, J.A. Riera, Phys. Rev. B **54**, 16032 (1996).
11. H. Fukuyama, T. Tanimoto, M. Saito, J. Phys. Soc. Jpn **65**, 1182 (1996).
12. D. Khomskii, W. Geertsma, M. Mostovoy, Czech. J. Phys. **46** (1996) Suppl S6, LT21 Conference Proceedings.
13. M. Fabrizio, R. Mélin, Phys. Rev. Lett. **78**, 3382 (1997).
14. M. Fabrizio, R. Mélin, Phys. Rev. B **56**, 5996 (1997).
15. M. Fabrizio, R. Mélin, J. Souletie, Eur. Phys. J. B **10**, 607 (1999).
16. A. Dobry, P. Hansen, J. Riera, D. Augier, D. Poilblanc, Phys. Rev. B **60**, 4065 (1999).
17. M. Laukamp, G.B. Martins, C. Gazza, A.L. Malvezzi, E. Dagotto, P.M. Hansen, A.C. López, J. Riera, Phys. Rev. B **57**, 10755 (1998).
18. P.M. Hansen, J.A. Riera, A. Delia, E. Dagotto, Phys. Rev. B **58**, 6258 (1998).
19. P. Hansen, D. Augier, J. Riera, D. Poilblanc, Phys. Rev. B **61**, 6741 (2000).
20. E. Sorensen, I. Affleck, D. Augier, D. Poilblanc, Phys. Rev. B **58**, R14701 (1998).
21. O. Motrunich, S.C. Mau, D.A. Huse, D.S. Fisher, Phys. Rev. B **61**, 1160 (2000).
22. B. Grenier, J.P. Renard, P. Veillet, C. Paulsen, R. Calemcsuk, G. Dhalenne, A. Revcolevschi, Phys. Rev. B **57**, 3444 (1998).
23. M. Saint-Paul, J. Voiron, C. Paulsen, P. Monceau, G. Dhalenne, A. Revcolevschi, J. Phys. Cond. Matt. **10**, 10215 (1998).
24. V. Kiryukin, B. Keimer, J.P. Hill, A. Vigliante, Phys. Rev. Lett. **76**, 4608 (1996).
25. M. Horvatić, Y. Fagot-Revurat, C. Berthier, G. Dhalenne, A. Revcolevschi, Phys. Rev. Lett. **83**, 420 (1999).
26. R.J. Baxter, *Exactly solved models in statistical mechanics* (Academic Press, 1982).
27. J.M. Carlson, J.T. Chayes, L. Chayes, J.P. Sethna, D.J. Thouless, J. Stat. Phys. **61**, 987 (1990)
28. D.S. Fisher, Phys. Rev. B **50**, 3799 (1994).
29. M. Mostovoy, D. Khomskii, J. Knoester, Phys. Rev. B **58**, 8190 (1998).
30. C. Dasgupta, S.K. Ma, Phys. Rev. B **22**, 1305 (1980).
31. R.N. Bhatt, P.A. Lee, Phys. Rev. Lett. **48**, 344 (1982).
32. R. A. Hyman, K. Yang, R.N. Bhatt, S.M. Girvin, Phys. Rev. Lett. **76**, 839 (1996).
33. R.A. Hyman, K. Yang, Phys. Rev. Lett. **78**, 1783 (1997).
34. C. Monthus, O. Golinelli, Th. Jolicoeur, Phys. Rev. Lett. **79**, 3254 (1997)
35. E. Westerberg, A. Furusaki, M. Sigrist, P.A. Lee, Phys. Rev. B **55**, 12578 (1997).